JOURNAL OF MATERIALS SCIENCE 26 (1991) 6618–6624

Density and microstructure of CVD SiC–C nanocomposites

Y. WANG, M. SASAKI, T. HIRAI
Institute for Materials Research, Tohoku University, Katahira 2-1-1, Aobaku, Sendai 980, Japan

Density, microstructure and preferred crystal orientation of CVD SiC–C nanocomposites were studied for every composition from SiC to C. The relationships between these properties are discussed. The CVD SiC prepared in this work was dense with its density close to the theoretical value. However, some pores were formed by addition of dispersed C. The densities of CVD C were as low as about 80% of the theoretical value. The densities approached close to the theoretical density by adding a small amount of SiC. The preferred crystal orientations parallel to the substrate were (1 1 0) or (1 1 1) for CVD SiC and (0 0 2) for CVD C. When the quantity of dispersion phases exceeds a certain value, a decrease in the preferred orientation is found for both SiC and C matrices and the formation of pores becomes much easier.

1. Introduction

In recent years, the development of materials which can be utilized under severe temperature conditions as experienced in the aerospace and nuclear fusion technologies has been undertaken. One of the approaches in this development is the preparation of "nanocomposites" in which a second phase of nanometre size is dispersed in the matrix [1]. Among these the material receiving considerable attention is the so called "functionally gradient material" [2, 3] in which the material properties are continuously changed by gradually varying the dispersion to matrix ratio from one surface of the material to the other surface.

Chemical vapour deposition (CVD) technique is an effective approach in fabricating nanocomposites and functionally gradient material through a codeposition process using multi-component gas reactions [4, 5]. The main advantage of the CVD technique is its ease of controlling the composition and microstructure of the deposited materials.

Recently, a functionally gradient material consisting of silicon carbide (SiC) and carbon (C) prepared by CVD was examined as a thermal barrier for a space plane [6] due to its excellent oxidation resistance and good thermal shock resistance. To design and prepare the CVD SiC/C functionally gradient material, it is necessary to study the relationships between composition, microstructure and properties of CVD SiC–C nanocomposites for every composition. However, the preparation of SiC–C nanocomposites having its composition (C/(SiC + C)) over the entire range of SiC to C has not been attempted.

Investigators are conducting studies on CVD SiC–C nanocomposites for every composition prepared by use of $SiCl_4$–C_3H_8–H_2 and attempting to find the relationships among the deposition conditions, composition, microstructure and properties. We have reported in our earlier paper [7] concerning the proper CVD conditions for the preparation of dense-plate SiC–C nanocomposites. These deposition conditions were obtained by thermodynamic calculation and deposition experiment. In the present work, density, microstructure and preferred crystal orientation of CVD SiC–C nanocomposites were studied and the relationships among these properties are discussed.

2. Experimental procedure

The preparation method of CVD SiC–C nanocomposites has been reported in a previous paper [7]. A graphite substrate (40 mm × 12 mm × 2 mm) placed in a cold-wall reactor was heated by an electric current. $SiCl_4$, C_3H_8 and H_2 were used as source gases. The C_3H_8 gas flow rate was kept constant. $SiCl_4$ reservoir was kept at 293 K and its vapour was transported into the furnace by bubbling hydrogen carrier gas. The molar ratios of Si to C ($m_{Si/C}$) in the input gas were changed by controlling $H_2(SiCl_4)$ vapour flow rate. The deposition conditions are shown in Table I.

The free-carbon contents in the deposits were determined by chemical analysis in which powdered samples were burnt in oxygen at 1073 K and the CO_2 gas thus formed was titrated by coulometry. The density of the deposits was determined by Archimedes' principle. In order to accurately measure the density of the deposits containing pores, the actual density measure-

TABLE I CVD conditions

Deposition temperature,	T_{dep}(K):	1673, 1773, 1873
Total gas pressure,	P_{tot}(kPa):	6.7, 13.3, 40
Gas flow rate (10^{-6} m^3 s^{-1}),	H_2:	0 to 11.7
	$SiCl_4$:	0 to 3.9
	C_3H_8:	0.67
Si to C ratio in input gas,	$m_{Si/C}$:	0 to 1.9
Deposition time,	t_{dep}(ks):	3.6

0022–2461/91 $03.00 + .12

ment was made after varnishing the samples. Microstructure was investigated by a scanning electron microscope (SEM) (Akashi: ALPHA-30W). An X-ray diffractometer (Rigaku: RAD-IIB) was used to measure the degree of preferred crystal orientation parallel to the substrate for SiC and C. Electrical conductivity of CVD SiC–C nanocomposites was measured by four point direct current method.

3. Results

3.1. Density

Fig. 1 shows the change in composition of CVD SiC–C nanocomposites with $m_{Si/C}$ of input gas. These deposits were prepared at the conditions of Table I. The compositions change continuously from C to SiC with the increase of the $m_{Si/C}$ in the input gas [7]. The deposits were able to be categorized into "dense-plate" deposits and "porous" deposits. The conditions where the dense-plate were formed are shown as blocks in Fig. 2. As shown by continuous blocks in Fig. 2, at the conditions of T_{dep} = 1673 K and P_{tot} = 6.7 to 40 kPa and at T_{dep} = 1773 K and P_{tot} = 40 kPa, dense-plate deposits are formed at all the $m_{Si/C}$ range examined. The densities of the deposits formed in these conditions are shown in Fig. 3. The theoretical densities of the deposits shown by a broken line in Fig. 3 were calculated by use of the mixture rule and the theoretical density of SiC (3.2×10^3 kg m^{-3}) and C (2.26×10^3 kg m^{-3}). The densities of CVD SiC agree fairly well with the theoretical value, however, the density of CVD SiC–C composites was lower than their theoretical value. The densities of CVD C are 1.64 to 1.85 $\times 10^3$ kg m^{-3} and as low as about 80% of their theoretical values which were calculated from their lattice parameters. The densities reached as high as 1.95 to 2.15 $\times 10^3$ kg m^{-3} by adding SiC (< 5 mol %)

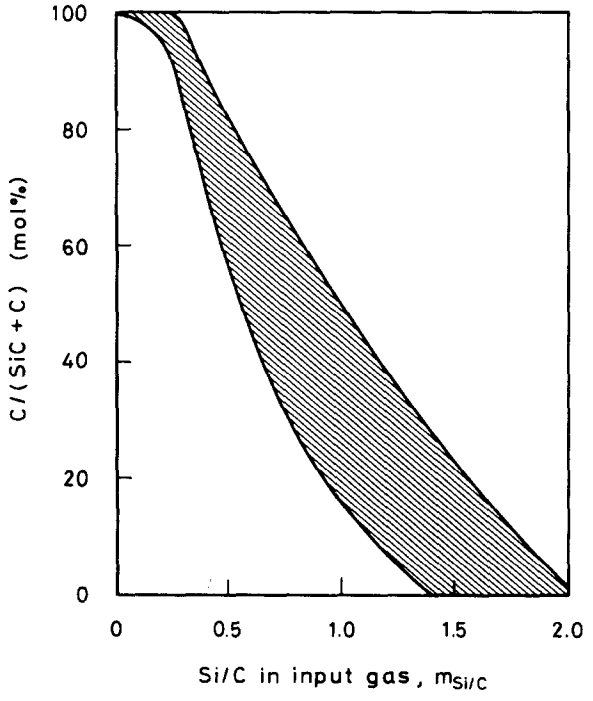

Figure 1 Relationship between the composition of deposits and Si/C molar ratio in input gas (T_{dep} = 1673 to 1873 K, P_{tot} = 6.7 to 40 kPa).

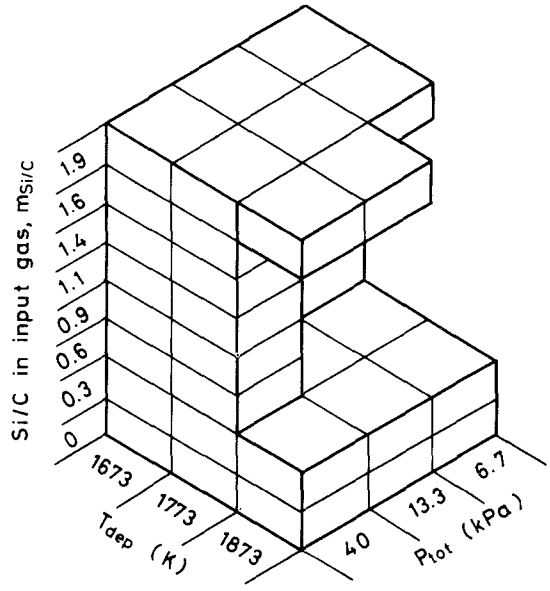

Figure 2 Deposition conditions for SiC–C dense plates.

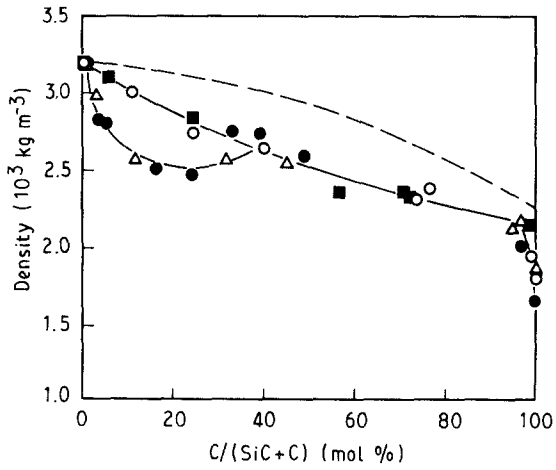

Figure 3 Relationship between density and composition. T_{dep}, P_{tot}: (●) 1673 K, 6.7 kPa; (△) 1673 K, 13.3 kPa; (○) 1673 K, 40 kPa; (■) 1773 K, 40 kPa; and (---) calculated.

in CVD C. These values are much closer to the theoretical density than what were measured for a single phase C. This result suggests that the deposition of a small quantity of SiC can densify the resulting product.

Fig. 3 shows that in the composition range up to 25 mol % C, the deposits formed at P_{tot} = 6.7 to 13.3 kPa have a significantly lower density than those formed at P_{tot} = 40 kPa. Even for the deposits formed at P_{tot} = 40 kPa, the difference in the densities between the experiment and the calculation increases with an increase of dispersion phases (SiC or C). The density of the deposit containing 56.6 mol % C was about 85% of the calculated value.

3.2. Microstructure

Fig. 4a to c show the SEM micrographs of deposition surface for CVD SiC formed at T_{dep} = 1673 to 1873 K and P_{tot} = 40 kPa. The CVD SiC deposited at T_{dep} = 1673 K showed a fine pebble structure (Fig. 4a). When T_{dep} = 1773 K, the size of their pebbles (Fig. 4b)

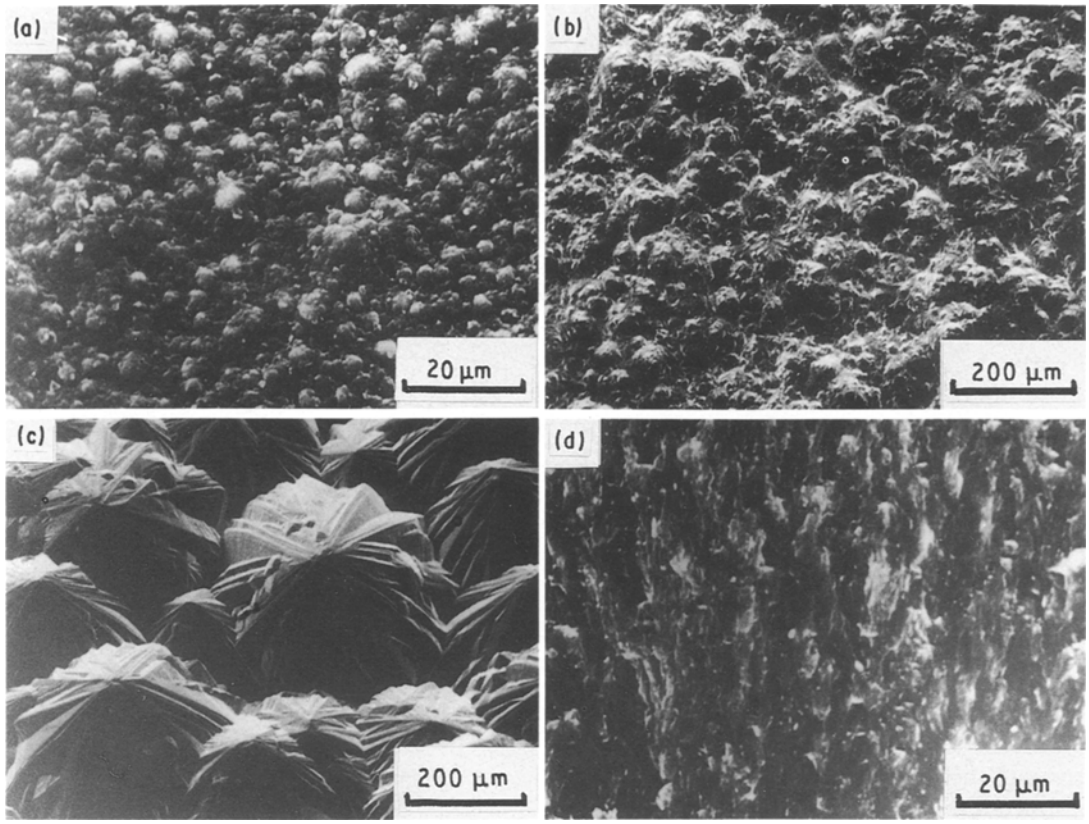

Figure 4 Scanning electron micrographs of CVD SiC prepared at P_{tot} = 40 kPa and (a) T_{dep} = 1673 K, deposited surface, (b) T_{dep} = 1773 K, deposited surface, (c) T_{dep} = 1873 K, deposited surface, (d) T = 1673 K, cross-sectional surface.

amounts to ten times the ones formed at T_{dep} = 1673 K. The structure changes to an advanced facet structure at T_{dep} = 1873 K (Fig. 4c). Though there are some differences in cross-sectional surfaces for CVD SiC formed at different deposition temperatures, they are all columnar structures with their axes perpendicular to the substrate. Fig. 4d shows an example of this structure.

Fig. 5 shows the cross-sectional surface structure of CVD SiC–5.8 mol % C. With the introduction of dispersed C phase, fine pores begin to form at the boundary of SiC crystals. Fig. 6 shows the cross-sectional surface of CVD SiC–24.3 mol % C. The SiC crystals are flake-like and have no preferred growth direction. At the boundary between the flakes having different growth direction, pores of the size about 1 μm can be observed. Fig. 7 shows the cross-sectional surface of CVD SiC–71 mol % C, where fine crystals of SiC and C had a dendritic structure. Within these dendrites and at their boundaries as much as 12 vol % pores were observed. It is noted that some parts of C phase in the deposit have a layer structure.

Figs 8 and 9 show the cross-sectional surface of CVD SiC–98.5 mol % C and 100% CVD C, respectively. All of them show a layer structure with their layer plane parallel to the substrate. The general structural arrangement of CVD SiC–98.5 mol % C is much more regular than that of CVD C.

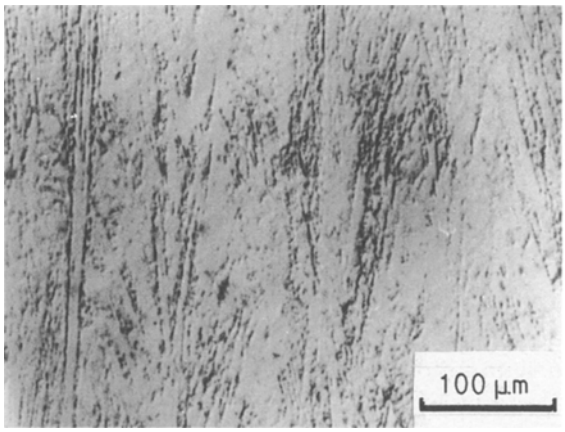

Figure 5 Optical micrograph of polished cross-sectional surface of CVD SiC–5.8 mol % C (T_{dep} = 1773 K, P_{tot} = 40 kPa).

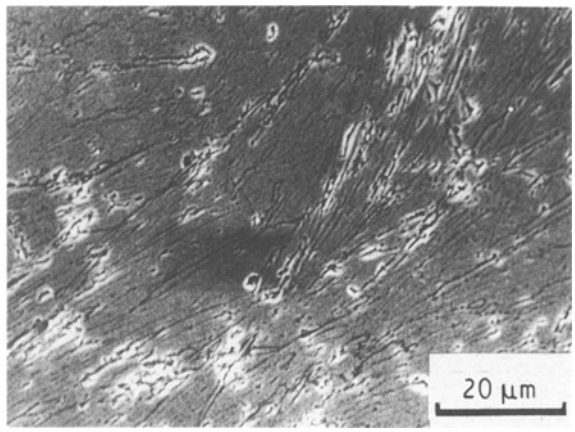

Figure 6 Scanning electron micrograph of polished cross-sectional surface of CVD SiC–24.3 mol % C (T_{dep} = 1773 K, P_{tot} = 40 kPa).

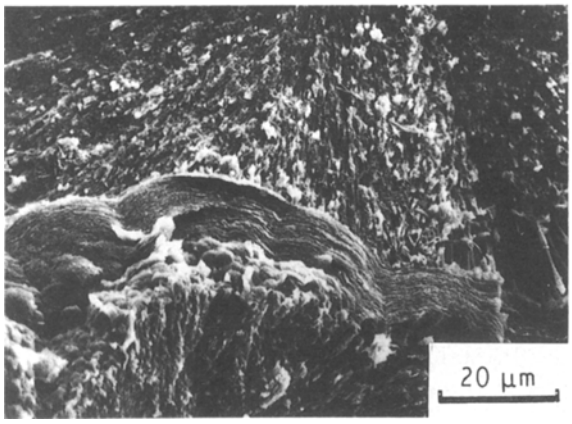

Figure 7 Scanning electron micrograph of cross-sectional surface of CVD SiC–71.0 mol % C (T_{dep} = 1773 K, P_{tot} = 40 kPa).

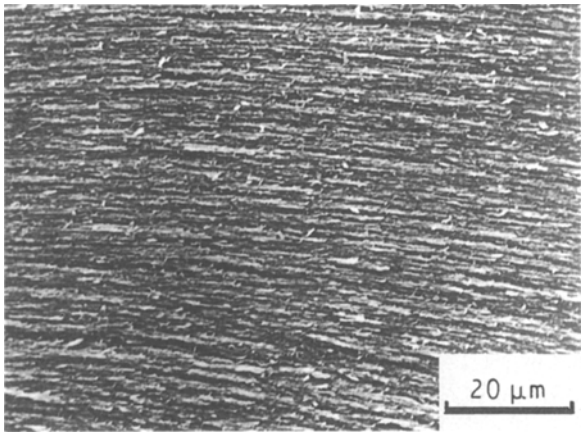

Figure 8 Scanning electron micrograph of cross-sectional surface of CVD SiC–98.5 mol % C (T_{dep} = 1773 K, P_{tot} = 40 kPa).

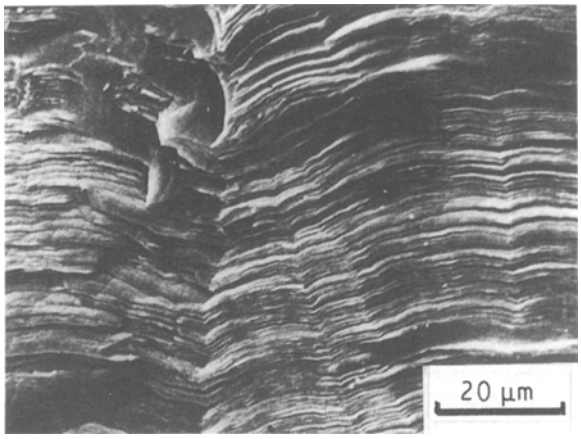

Figure 9 Scanning electron micrograph of cross-sectional surface of CVD C (T_{dep} = 1773 K, P_{tot} = 40 kPa).

The deposits so far shown in Figs 5 to 9 are all formed at T_{dep} = 1773 K and P_{tot} = 40 kPa. For the deposits formed at T_{dep} = 1673 K and P_{tot} = 40 kPa, their microstructure was generally similar to the one formed at T_{dep} = 1773 K and P_{tot} = 40 kPa but had a more homogeneous structure. Furthermore, even for CVD SiC–73.5 mol % C formed at T_{dep} = 1673 K, layered C as shown in Fig. 7 was not observed.

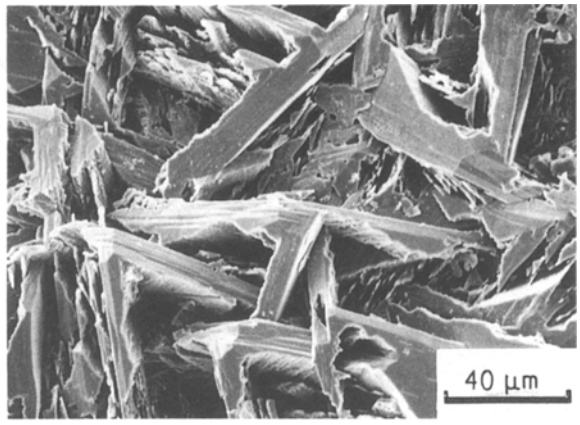

Figure 10 Scanning electron micrograph of deposited surface of CVD SiC–3.3 mol % C (T_{dep} = 1673 K, P_{tot} = 13.3 kPa).

The deposits formed at P_{tot} = 6.7 to 13.3 kPa had more large scale structure than that formed at P_{tot} = 40 kPa and contained large pores as shown in Fig. 10. This observation agrees well with the earlier result that the deposits formed at P_{tot} range of 6.7 to 13.3 kPa and having C contents of up to 25 mol % had lower densities (Fig. 3).

3.3. Preferred crystal orientation

X-ray diffraction clearly showed that SiC–C nanocomposites prepared in this work consisted of a cubic SiC and a hexagonal planar carbon. Generally, CVD C tend to lie on the substrate by their (0 0 2) planes [8] and cubical CVD SiC by their (1 1 0) or (1 1 1) planes [9]. In this work, the same preferred orientations were found. CVD SiC formed at T_{dep} = 1673 K and P_{tot} = 40 kPa showed (1 1 1) plane, while at the other deposition conditions it showed (1 1 0) plane.

Having the data of X-ray diffraction, the degree of preferred orientation for SiC contained in the CVD SiC–C nanocomposites (T_{SiC}) is calculated by the equation [10]

$$T_{SiC}(h\,k\,l) = \frac{I_b(h\,k\,l)/I_p(h\,k\,l)}{(1/n)\sum_n I_b(h\,k\,l)/I_p(h\,k\,l)} \quad (1)$$

where I_b and I_p are X-ray diffraction intensity of bulk and powder samples, respectively, and n is the number of diffractions. The degree of preferred orientation for C in CVD SiC–C nanocomposites (T_C) is calculated by the equation.

$$T_C(0\,0\,2) = \frac{180^\circ}{W} \quad (2)$$

where W is the half-value width (degree) of inclination angle of $(0\,0\,2)_C$ obtained from X-ray diffraction intensity distribution that was measured by rotating a stick-like specimen for a fixed diffraction angle 2θ [11]. In the calculations using Equations 1 and 2, random oriented crystals for both SiC and C are signified when T = 1.

Fig. 11 shows the variation for the preferred orientation degree of SiC with the composition and

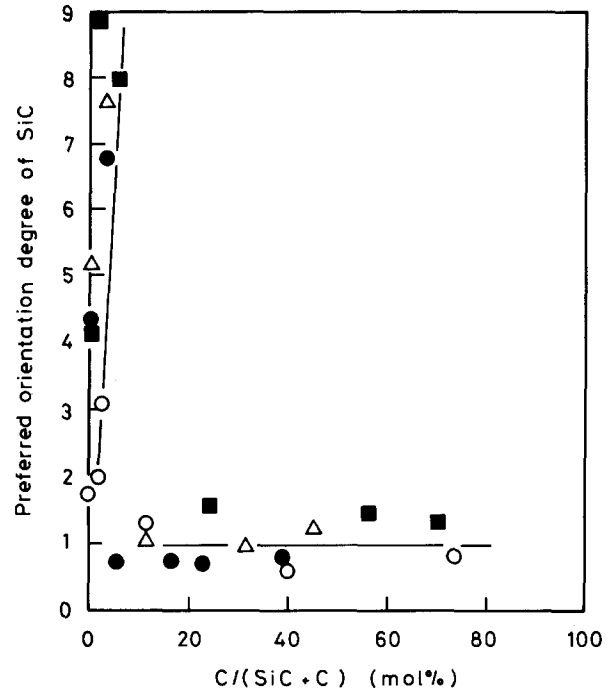

Figure 11 Effect of the composition on the preferred orientation of SiC crystallites contained in CVD SiC–C nanocomposites. T_{dep}, P_{tot}: ●: (1 1 0), 1673 K, 6.7 kPa; △: (1 1 0), 1673 K, 13.3 kPa; ○: (1 1 1), 1673 K, 40 kPa; ■: (1 1 0), 1773 K, 40 kPa.

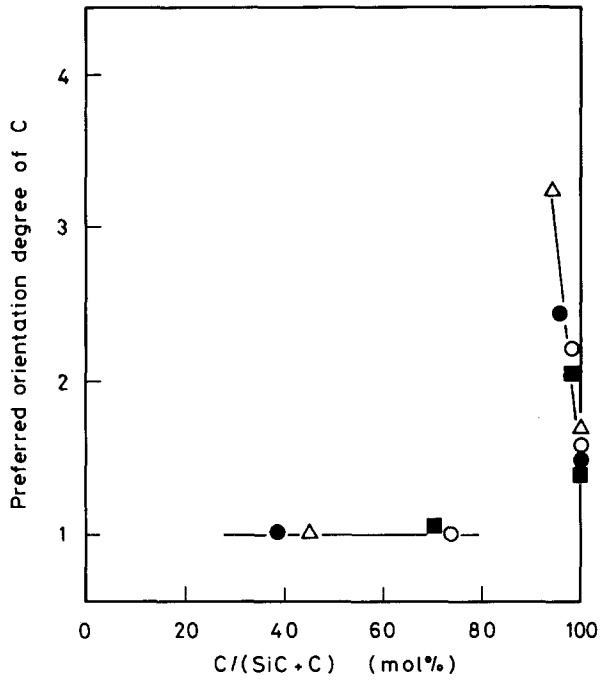

Figure 12 Effect of the composition on the preferred orientation of C crystallites contained in CVD SiC–C nanocomposites. T_{dep}, P_{tot}: (●) 1673 K, 6.7 kPa; (△) 1673 K, 13.3 kPa; (○) 1673 K, 40 kPa; (■) 1773 K, 40 kPa.

Fig. 12 shows that of C. From Figs 11 and 12, it can be seen that the preferred orientation degree of SiC and C is very high when a little dispersion phase existed, but the orientations disappear quickly as the dispersion phase contents increases.

4. Discussion

4.1. Density

When the deposition temperature is in the range lower than 2000 K, the resulting CVD C is known to show lower density than the theoretical value [12, 13]. Hirai and Yajima reported that 45 vol % of inter-crystallite pores are contained for a low density CVD C sample [14]. The presence of pores was also demonstrated by the results of X-ray small angle scattering [15].

Yajima and Hirai [16] and Marinković *et al.* [17] reported the improvement in the density of CVD C by adding a small amount of SiC dispersion phase in C matrix. Yajima and Hirai prepared CVD C–SiC (< 2 mol % SiC) at T_{dep} = 1673 to 2273 K and reported that the densities were higher than that of CVD C. In addition, the minimum density that appeared in CVD C at near T_{dep} = 1900 K was not found in CVD C–SiC [16]. Moreover, the crystal size in "a" axial direction and the preferred orientation degree of C matrix was greater than that of CVD C [18]. These results were explained as a consequence of graphitization of amorphous C existing in CVD C due to the catalysis effect of some intermediate products of Si-H-C-Cl system. Just as Yajima and Hirai [16], Marinković *et al.* [17] reported the density of CVD C deposited at T_{dep} = 1800 K was about 1.8 $\times 10^3$ kg m^{-3}, while that of CVD C–SiC (< 5 mol % SiC) was higher than 2.1 $\times 10^3$ kg m^{-3}. The results presented in this paper are in good agreement with these values.

Table II compared the structural parameters of CVD C and CVD C–1.5 mol % SiC prepared in this work. The interlayer spacing of C ($C_0/2$) in CVD C–1.5 mol % SiC is similar to that of CVD C as shown in Table II. However, both crystal size in "a" axial direction (L_a) and the preferred orientation degree (T_C) were considerably greater than that of CVD C. Thus, one may conclude that the improvement of the density by addition of SiC in CVD C is due to the progress in structural regularity of C matrix.

Kaae and Gulden [19], Bonnke and Fitzer [20] and Hirai *et al.* [21] have studied the density of CVD SiC–C nanocomposites in a relatively wide composition range. Fig. 13 compares their results with the present work. Though the deposition conditions and the source materials in each experiment was different, the results showed the same tendency, i.e., the relative density of CVD SiC–C decreased with increasing the content of the dispersion phases. This result implies that pores tend to be formed when C and SiC are combined to form a composite by CVD in a wide composition range. The cause of these pores formation has not been reported.

From the results of the present work, it was disclosed that single phase CVD SiC and CVD C possess a high degree of preferred orientation but as the content of the dispersion phase increases to a certain

TABLE II Characterization of C and C–1.5 mol % SiC

	C	C–1.5 mol % SiC
$C_0/2$ (nm)	0.344	0.342
L_a (nm)	3.83	7.46
T_C (0 0 2)	1.4	2.1

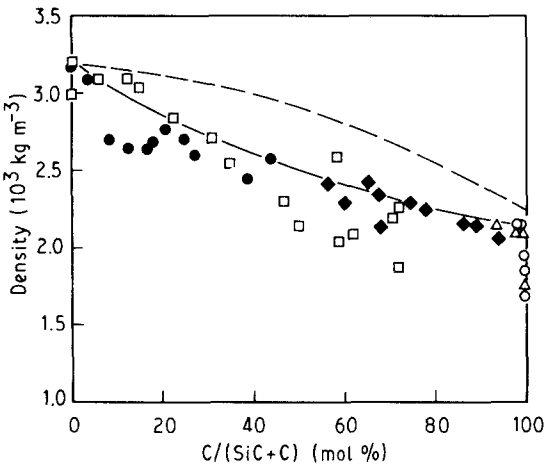

Figure 13 Comparison of density of CVD SiC–C prepared at different condition. (——) Present work; (○, △, ◆, □, ●) according to references [16, 17, 19–21] respectively; (---) calculated.

level the formation of both SiC and C lose orientation and take place in random fashion. Therefore, the cause of the density of SiC–C nanocomposites decrease with the increasing content of dispersion phases may be due to that pores are formed easily accompanying the irregular crystal growth. Though it is necessary to study further in detail the effects of the pores on the thermal and mechanical properties of the composites, one can anticipate the thermal shock resistance and thermal stress relaxation of CVD SiC–C nanocomposites should be improved due to the presence of the pores.

4.2. Microstructure

SiC monolith prepared in this work had a columnar structure with its axis perpendicular to the substrate, however, with an increase of C contents, SiC showed flack-like and fine crystals. Furthermore, the CVD C and CVD C–1.5 mol % SiC had a layer structure in the direction parallel to the substrate, and C phase had fine crystals as the quantity of SiC was increased. Fig. 14 illustrates these structures in a schematic diagram. The remarkable microstructure change with the composition as shown in Fig. 14 can be explained by the difference of the crystal structures and crystal growth features of SiC and C.

Yajima and Hirai [22] reported that SiC in CVD C–SiC (< 2 mol %) showed disc-like single crystals having the plane parallel to (0 0 2) planes of C. On the other hand, Muench and Pettenpaul [23] reported C dispersion phase contained in CVD SiC matrix tends to exist at the grain boundaries of SiC. Fig. 15 shows the relationship between the electrical conductivity and the composition of CVD SiC–C nanocomposites. The conductivity increased with increasing C contents rapidly. It signifies the C phase tends to form a continuous network and gives higher electrical conductivity. This result agrees with that in BN–C [24] and Si_3N_4–C [25] systems and can be related to the microstructure of CVD SiC–24.3 mol % C (Fig. 6) where continuous grain boundaries of SiC were observed on the polished surface for the C existence.

Up to now, only a few papers have reported on the microstructure of CVD SiC–C composites formed in a wide composition range. Bonnke and Fitzer [20] deposited CVD SiC–C in the range of 0 to 72 mol % C using $(CH_3)_xSiCl_{4-x}$–CH_4 system by hot-wall type reactor and reported SiC–30 mol % C had a layer structure piled upon by SiC and C crystals. Their results are consistent with the CVD SiC–24.3 mol % C prepared in this work. Kaae and Gulden [19] prepared SiC–C composite particles in a fluidized bed furnace using CH_3SiCl_3–C_3H_8–He system. They reported that SiC phase in C matrix was particle-like, and the size of SiC particles increased as the quantity increased from 5 to 45 mol % and gradually formed a continuously connected structure. In the present work a continuously connected structure due to the SiC particles was not identified. It is possible that characteristics of the microstructure of CVD SiC–C nanocomposites are affected not only by the composition but also by the furnace type and source materials.

5. Conclusions

Density and microstructure of SiC–C nanocomposites prepared by CVD using $SiCl_4$–C_3H_8–H_2 system at $T_{dep} = 1673$ K, $P_{tot} = 6.7$ to 40 kPa and $T_{dep} = 1773$ K, $P_{tot} = 40$ kPa were studied. The following results were obtained:

1. The density of CVD SiC agreed well with the theoretical value. However, pores were formed when C dispersion phase was introduced in SiC. The density of CVD C was as low as 80% of the theoretical value, and became more dense when added SiC was less than 5 mol %.

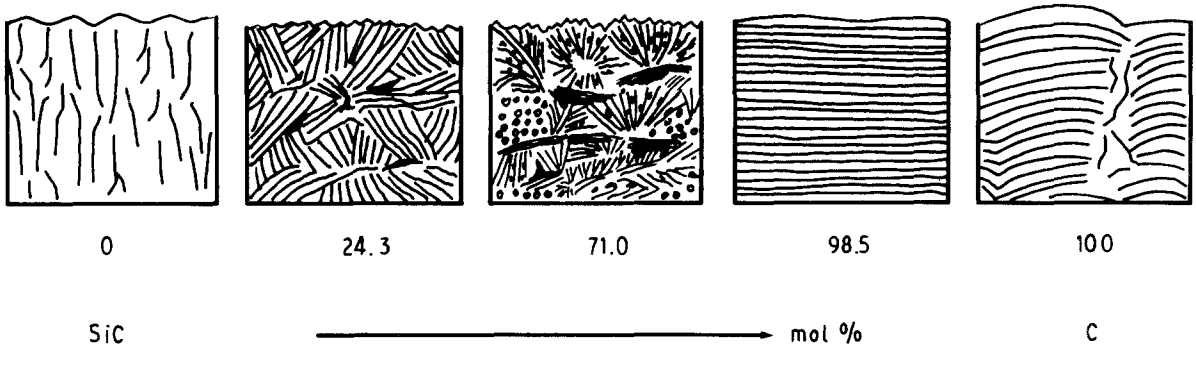

Figure 14 Schematic diagram of microstructure of CVD SiC–C nanocomposites.

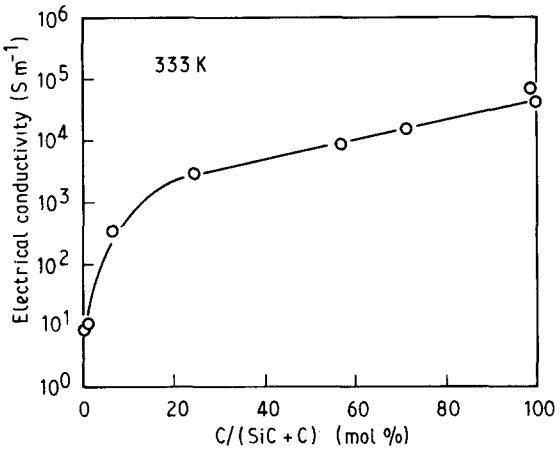

Figure 15 Electrical conductivity of CVD SiC–C nanocomposites (T_{dep} = 1773 K, P_{tot} = 40 kPa).

2. Morphology of SiC in CVD SiC–C nanocomposites changed from columnar to flack-like to fine crystals as the C contents was increased. CVD C and about 1.5 mol % SiC containing C both showed a layer structure with their plane parallel to the substrate. Whether C or SiC is the matrix the pores increased with the increase of dispersion phase.
3. Deposits containing up to 25 mol % C formed at P_{tot} = 6.7 to 13.3 kPa showed bulky structure and contained some large pores. Their densities were lower than those formed at P_{tot} = 40 kPa.
4. The preferred crystal orientation was such that (0 0 2) plane for CVD C and (1 1 0) or (1 1 1) plane for CVD SiC parallel to the substrate. The presence of a few dispersion phase strengthened the preferred orientation of the matrix, however, the matrix became randomly oriented when dispersion phase exceeded a certain level.

Acknowledgements

This research was supported in part by the Grant-in-Aid for Scientific Research from the Ministry of Education, Science and Culture, under Contract Nos. 63 850 149 and 63 750 730.

References

1. R. ROY, *Mater. Sci. Res.* **21** (1986) 25.
2. T. HIRAI, M. SASAKI and M. NIINO, *J. Soc. Mat. Sci. Jap.* **36** (1987) 1205.
3. M. NIINO, T. HIRAI and R. WATANABE, *J. Jap. Soc. Compos. Mat.* **13** (1987) 257.
4. T. HIRAI, "Emergent Process Methods for High Technology Ceramics", Materials Science Research Series, Vol. 17, edited by R. F. Davis, H. Palmour III and R. L. Porter (Plenum Press, New York, 1984) p. 329.
5. T. HIRAI and T. GOTO, "Tailoring Multiphase and Composite Ceramics", edited by R. E. Tressler, G. L. Messing, C. G. Pantano and R. E. Newnham (Plenum Press, New York, 1986) p. 165.
6. M. SASAKI, Y. WANG, T. HIRANO and T. HIRAI, *Nippon Seramikkusu Kyokai Gakujutsu Ronbonshi* **97** (1989) 539.
7. Y. WANG, M. SASAKI, T. GOTO and T. HIRAI, *J. Mat. Sci.* **25** (1990) 4607.
8. J. C. BOKROS, "Chemistry and Physics of Carbon", Vol. 5 edited by Philip L. Walker, Jr (Plenum Press, New York, 1969) p. 13.
9. J. SCHLICHTING, *Powder Met. Int.* **12** (1980) 141.
10. C. W. LEE, S. W. NAM and J. S. CHUN, *J. Vac. Sci. Technol.* **21** (1982) 42.
11. T. HIRAI, *Trans. Jap. Inst. Met.* **8** (1967) 190.
12. S. YAJIMA, T. SATOW and T. HIRAI, *J. Nucl. Mat.* **17** (1965) 127.
13. R. J. BARD, H. R. BAXMAN, J. P. BERTINO and J. A. O'ROURKE, *Carbon* **6** (1968) 603.
14. T. HIRAI and S. YAJIMA, *J. Mat. Sci.* **2** (1967) 18.
15. R. H. BRAGG, M. L. HAMMOND, J. C. ROBINSON and P. L. ANDERSON, *Nature* **200** (1963) 555.
16. S. YAJIMA and T. HIRAI, *J. Mat. Sci.* **4** (1969) 416.
17. S. MARINKOVIĆ, Č. SUŽNJEVIĆ, I. DEŽAROV, A. MIHAJLOVIĆ and D. CEROVIĆ, *Carbon* **8** (1970) 283.
18. S. YAJIMA and T. HIRAI, *J. Mat. Sci.* **4** (1969) 685.
19. J. L. KAAE and T. D. GULDEN, *J. Amer. Ceram. Soc.* **54** (1971) 605.
20. V. M. BONNKE and E. FITZER, *Ber. Dtsch. Keram. Ges.* **43 H.2** (1966) 180.
21. T. HIRAI, T. GOTO and T. KAJI, *Yogyo-Kyokai-Shi* **91** (1983) 502.
22. S. YAJIMA and T. HIRAI, *J. Mat. Sci.* **4** (1969) 424.
23. W. V. MUENCH and E. PETTENPAUL, *J. Electrochem. Soc.* **125** (1978) 294.
24. S. H. CHEN and R. J. DIEFENDORF, Proceedings of the 3rd International Carbon Conference (Pion London, 1981) p. 44.
25. T. GOTO and T. HIRAI, *J. Mat. Sci.* **18** (1983) 383.

Received 22 January
and accepted 30 November 1990